

Redox control of miRNAs and their targets in wheat

Jie Cao^{1a}, Zsolt Gulyás^{2a}, Balázs Kalapos^{2,3}, Ákos Boldizsár², Xinye Liu¹, Magda Pál²,
Yingyin Yao¹, Gábor Galiba^{2,3}, Gábor Kocsy^{2*}

¹State Key Laboratory for Agrobiotechnology and Key Laboratory of Crop Heterosis and Utilization, China Agricultural University, No. 2 Yuanmingyuan West Road, Haidian District, Beijing, China

²Agricultural Institute, Centre for Agricultural Research, Hungarian Academy of Sciences, 2462 Martonvásár, Brunszvik str. 2., Hungary

³Festetics Doctoral School, Georgikon Faculty, University of Pannonia, 8360 Keszthely, Deák Ferenc str. 16., Hungary,

^aThese authors contributed equally to this work.

*Corresponding author, e-mail: kocsy.gabor@agrar.mta.hu, phone number: +3622569501

e-mail addresses of the other authors:

JC: cao2014jie@163.com

ZG: gulyas.zsolt@agrar.mta.hu

BK: kalapos.balazs@agrar.mta.hu

ÁB: boldizsar.akos@agrar.mta.hu

XL: 419405014@qq.com

MP: pal.magda@agrar.mta.hu

YY: yingyin@cau.edu.cn

GG: galiba.gabor@agrar.mta.hu

Date of submission:

Number of figures: 10

Figures should be colour in print: Fig. 1, Fig. 6, Fig. 9

Word count: 7364, max 6500

Number of supplementary figures: 7

Number of supplementary tables: 8

1 **Running title:** Redox control of miRNAs in wheat

2

3 **Highlight**

4 A redox-dependent regulatory network of miRNAs and their targets were created using
5 sequencing results, bioinformatics tools and correlation analysis of the examined biochemical
6 and molecular parameters in wheat.

7

8 **Abstract**

9 Possible redox control of miRNAs was investigated in wheat. One-day treatment of seedlings
10 with 10 mM H₂O₂ resulted in decreased glutathione content and increased half-cell reduction
11 potential of the glutathione disulphide/glutathione redox pair and greater ascorbate peroxidase
12 activity compared to the control plants. These changes were accompanied by alterations in the
13 miRNA transcript profile, since 70 miRNAs with at least 1.5-fold difference in their
14 expression between control and treated (0, 3, 6 h) seedlings were identified. Their 86 target
15 genes were determined by degradome sequencing and 6808 possible additional target genes
16 were identified by bioinformatics tools. The H₂O₂-responsiveness (24 h treatment) of 1647
17 targets was also confirmed by transcriptome analysis. They are mainly related to the control
18 of redox processes, transcription and protein phosphorylation and degradation. In a time-
19 course experiment (0, 1, 3, 6, 9, 12, 24 h treatment) a correlation was found between the
20 levels of glutathione, other antioxidants and the transcript levels of the H₂O₂-responsive
21 miRNAs and their target mRNAs. This relationship together with the bioinformatics
22 modelling of the regulatory network indicate the glutathione-related redox control of miRNAs
23 and their targets, which allows the adjustment of the metabolism to changing environmental
24 conditions.

25

26 **Key words:** Ascorbate, glutathione, hydrogen-peroxide, miRNAs, redox regulation, wheat.

27 **Abbreviations:** AsA: ascorbic acid, APX: ascorbate peroxidase, CAT: catalase, GR:
28 glutathione reductase, GSH: glutathione, GSSG: glutathione disulphide, GST: glutathione S-
29 transferase, ROS: Reactive oxygen species.

30

31 **Introduction**

32 Reactive oxygen species (ROS) and antioxidants have an important role in the regulation of
33 growth and development both under optimal and stress conditions (Kocsy *et al.*, 2013;
34 Considine and Foyer, 2014; Locato *et al.*, 2018). Among ROS, H₂O₂ is the most stable ROS,
35 which makes it appropriate for long distance signalling and controlling of various metabolic
36 processes at the level of gene expression and protein activity (Foyer *et al.*, 1997; Neill *et al.*,
37 2002; Hossain *et al.*, 2015). Consistent with this hypothesis, increased H₂O₂ in catalase-
38 deficient *Arabidopsis thaliana* (L.) Heynh. mutants resulted in the induction of genes related
39 to the regulation of stress response, metabolism, development and energy homeostasis
40 (Vandenabeele *et al.*, 2004). In H₂O₂-treated *Arabidopsis*, altered expression of genes
41 encoding proteins involved in the transcription, signal transduction, protein transport, energy
42 homeostasis, cellular organisation and defence processes was observed by microarray analysis
43 (Desikan *et al.*, 2001). Similarly to *Arabidopsis*, genes involved in cell defence, signal
44 transduction and metabolism (carbohydrates and lipids) were also affected by H₂O₂ treatment
45 in wheat (Li *et al.*, 2011). Besides these genes, the expression of redox homeostasis- and
46 photosynthesis-related genes also changed in wheat. By a proteomic approach, the effect of
47 exogenous H₂O₂ on most of these processes was also shown in rice (Wan and Liu, 2008).
48 Besides its effect on the total amount of proteins, H₂O₂ may also regulate their activity due to
49 the oxidation of the Cys residues. The amount of H₂O₂ is regulated by the ascorbate-
50 glutathione (AsA-GSH) cycle which is composed of both enzymatic and non-enzymatic
51 components affecting indirectly the H₂O₂-dependent physiological processes (Roach *et al.*,
52 2018). Recently, the direct regulatory role of AsA and GSH was shown to modify the
53 development of reproductive organs and tolerance to low temperature through their effect on
54 redox system and gene expression (Gulyás *et al.*, 2014).

55 Similarly to the AsA-GSH cycle, microRNAs (miRNAs) are also important in the
56 control of development (Kidner and Martienssen, 2005; Rubio-Somoza and Weigel, 2011)
57 and stress response (Phillips *et al.*, 2007; Khraiwesh *et al.*, 2012; Rajwanshi *et al.*, 2014).
58 They can control the expression level of their target genes transcriptionally by DNA
59 methylation and post-transcriptionally by cleavage or translational inhibition of target
60 mRNAs. Many of the target genes of miRNAs encode transcription factors; therefore, one
61 miRNA is able to regulate indirectly a whole set of genes. miRNAs have a pleiotropic effect
62 in the control of development, but one target gene may also be regulated by more miRNAs
63 (Kidner and Martienssen, 2005). They are components of regulatory networks that coordinate

64 gene expression programs ensuring developmental plasticity (Rubio-Somoza and Weigel,
65 2011). Such network was described for developmental phase transitions, leaf senescence, cell
66 proliferation and leaf polarity; furthermore the interconnection of miRNA-dependent
67 regulatory networks has also been suggested under both biotic and abiotic stresses (Rajwanshi
68 *et al.*, 2014). In wheat, many miRNAs related to development and stress response were
69 discovered (Yao and Sun, 2012) either by computational approach (Dryanova *et al.*, 2008) or
70 by next generation sequencing (Sun *et al.*, 2014). Although miRNAs are evolutionarily
71 conserved, several monocot- or wheat-specific miRNAs were described. By surveying
72 miRNA profile in 11 different tissues, 323 novel miRNAs (belonging to 276 families) and
73 524 targets for 124 miRNAs were identified in a recent study of wheat (Sun *et al.*, 2014).
74 When the redox regulation of miRNAs was studied in rice, 7 H₂O₂-responsive miRNAs were
75 identified that are involved in transcriptional regulation, nutrient transport, auxin homeostasis,
76 cell proliferation and programmed cell death (Li *et al.*, 2011). In *Brachypodium distachyon*
77 (L.) P. Beauv. 61 H₂O₂-responsive miRNAs were determined the target of which were related
78 to development, reproduction, response to stress, secondary metabolism, catabolic processes,
79 nucleic acid metabolism and cellular component organization (Lv *et al.*, 2016).

80 The aim of the present study was to find out whether the effect of H₂O₂-induced
81 oxidative stress on miRNAs and their target genes is mediated by the GSH and other
82 antioxidants in wheat. For these purpose the determination of the H₂O₂-reponsive miRNA and
83 target mRNA profiles and regulatory networks were planned. The proposed relationship
84 between the various antioxidants and the levels of several miRNAs and their targets were
85 checked in a time course experiment.

86

87 **Materials and methods**

88 *Plant material and treatments*

89 Seeds of the wheat variety *Triticum aestivum* L. ssp. *aestivum* cv. *Chinese Spring* (CS) were
90 germinated in Petri dishes (1 day at 25°C, 3 days at 4°C, 2 days at 25°C). Seedlings were
91 grown on half-strength modified Hoagland solution with a photoperiod of 16 h, at 260 µmol
92 m⁻² s⁻¹, 22 °C and 75% RH in a growth chamber (Conviron PGV-15; Controlled Env., Ltd.,
93 Winnipeg, Canada) (Kocsy *et al.*, 2000). After 10 days of growth (2-leaf developmental
94 stage), 10 mM H₂O₂ was added to the nutrient solution and sampling was done after 0- (8 h
95 light), 1- (9 h light), 3- (11 h light), 6- (14 h light), 9- (1 h dark), 12- (4 h dark) and 24-hour (8
96 h light) treatments. The first sampling of leaves was performed in the middle of the 16-hour

97 light period in order to exclude the possible rapid changes that might occur in certain
98 examined parameters just after switching on the light. Besides the collection of leaf samples
99 (2nd leaves from the basis of the stem) for biochemical and molecular biological analysis, the
100 fresh and dry weights of the shoots and roots were also determined.

101

102 *Measurement of H₂O₂ content*

103 H₂O₂ content of the leaves was measured by FOX1 method using a spectrophotometer in a
104 colorimetric reaction as described in a previous study (Kellős et al., 2008). During this
105 reaction ferrous ion is oxidised to ferric ion by H₂O₂ and the ferric ion is detected by xylenol
106 orange.

107

108 *Determination of AsA*

109 Leaf samples of 500 mg fresh weight were ground with liquid nitrogen in a mortar and
110 extracted with 3 ml of 5% meta-phosphoric acid. In the supernatant, reduced and total AsA
111 (the latter reduced by dithiothreitol) contents were determined by HPLC using an Alliance
112 2690 system equipped with a W996 photodiode array detector (Waters, Milford, MA, USA).
113 The concentration of dehydroascorbate (DHA), a two-electron oxidized form of AsA was
114 estimated by subtracting the reduced portion from the total AsA pool (Szalai *et al.*, 2014).

115

116 *Analysis of cysteine and glutathione*

117 The leaves were ground with liquid nitrogen in a mortar, after which 1ml of 0.1 M HCl was
118 added to 200 mg plant sample. The total cysteine and glutathione pools (reduced + oxidised
119 forms) were determined after reduction with dithiothreitol and derivatisation with
120 monobromobimane (Kocsy *et al.*, 2000). For the detection of cystine and glutathione
121 disulphide (GSSG), cysteine and GSH were blocked with N-ethylmaleimide, after which the
122 excess of N-ethylmaleimide was removed with toluol (Kranner and Grill, 1996). Cystine and
123 GSSG were reduced and derivatised as described for total cysteine and glutathione pools. The
124 two thiols were analysed by an Alliance 2690 HPLC system using a W474 scanning
125 fluorescence detector (Waters, Milford, MA, USA). The amount of reduced thiols was

126 calculated as the difference between the amount of total and oxidised thiols. The half-cell
127 reduction potential of the thiol redox couples was calculated by the Nernst equation (Schafer
128 and Buettner, 2001).

129

130 *Analysis of the activity of the antioxidant enzymes*

131 The activities of catalase (CAT, EC 1.11.1.6; basis: reduction of H₂O₂), ascorbate peroxidase
132 (APX, EC 1.11.1.11; basis: reduction of H₂O₂ by AsA), glutathione reductase (GR, EC
133 1.6.4.2; basis: reduction of GSSG by NADPH and reaction of the produced GSH with 5-5"-
134 dithio- bis (2-nitrobenzoic acid)) and glutathione S-transferase (GST, EC 2.5.1.18; basis:
135 reaction of GSH with 1-chloro-2,4-dinitrobenzene) were determined in the leaves by
136 spectrophotometer using a colorimetric method as described previously (Soltész *et al.*, 2011).
137 The extraction buffer contained 1 mM AsA in order to avoid the inactivation of chloroplastic
138 APX as suggested by Noctor *et al.* (2016). The protein content was measured using Bradford-
139 reagent (Bradford, 1976) according to Soltész *et al.*, (2011).

140

141 *Small RNA sequencing*

142 Total RNA was isolated from the leaves of plants treated for 0-, 3- and 6-h with 10 mM H₂O₂
143 using the TRIzol reagent (Invitrogen, USA) according to the manufacturer's instructions. All
144 small RNA libraries prepared for this study according to Sun *et al.* (2014) were sequenced
145 with Illumina Hiseq 2000, generating approximately 10 M data for each sample. Low-quality
146 reads and portions of reads were removed using sickle program
147 (<https://github.com/najoshi/sickle>) with the parameters "-q 20 -f sanger -l 20". The cutadapt
148 program (Martin, 2011) was used to trim the 3' adaptors from reads (parameters "-
149 CTGTAGGCACCATCAATCAG - match-read-wildcards -m15"), and only the reads ranging
150 from 18 to 30 nucleotides were collected. Reads were then aligned to the Rfam 10.0 RNA
151 family database (Griffiths-Jones *et al.*, 2003; Griffiths-Jones, 2004; Nawrocki *et al.*, 2015)
152 with bowtie2 (Langmead and Salzberg, 2012) and known cellular structural RNAs, such as
153 rRNAs, tRNAs, snoRNAs, and snRNAs were removed based on their alignments using in-
154 house Perl script. The remaining reads were mapped to wheat microRNAs (Sun *et al.*, 2014)
155 collected and characterised by BLASTN and allowing no mismatches. The miRNA frequency

156 was normalised as "transcripts per million" (TPM), and the expression was set to 0.01 for
157 miRNAs that were not expressed in one of the samples after normalisation.

158 Following the first filtering for reliability, the differentially expressed miRNAs were
159 obtained by Bayes-based Poisson Distribution Test (Audic and Claverie, 1997) with
160 difference >1.5 times and sequencing reads >10 in at least one sample.

161

162 *Analysis of miRNAs by qRT-PCR*

163 Total RNA was isolated from frozen leaves using Trizol (Invitrogen, USA). The Mir-X
164 miRNA First-Strand Synthesis Kit (Clontech Laboratories, Inc) and SYBR Premix EX Taq II
165 (TaKaRa, Dalian, China) were used for miRNA reverse transcription and qRT-PCR according
166 to the manufacturer's instructions. qRT-PCR was performed on the CFX96 Real Time System
167 (BIO-RAD, USA) with the following program: denaturation at 95°C for 3 min, and then
168 subjected to 40 cycles of 95°C for 15 s, 60°C for 15 s, 72°C for 10 s. The entire sequence of
169 the mature miRNA (21–23 nt) was used as a miRNA-specific 5' primer. The 3' primer for the
170 qPCR was the mRQ 3' primer supplied with the kit. The relative expression of miRNA was
171 calculated using the $2^{-\Delta CT}$ method normalised to wheat *ACTIN* gene CT value. For each
172 sample, the PCR amplification was repeated three times, and the average values of $2^{-\Delta CT}$ were
173 used to determine the differences of gene expression by the Student's *t*-test. Three biological
174 replications were performed with similar results and one replicate was shown.

175

176 *Degradome sequencing*

177 Total RNAs obtained from leaves taken after 0 h, 3 h and 6 h H₂O₂ treatment were mixed
178 equally for degradome sequencing to see which miRNA targets are cleaved at any time point.
179 The degradome library was constructed briefly as followed: annealing of approximately 150
180 ng poly(A)-enriched RNA with Biotinylated Random Primers; Strapavidin capture of RNA
181 fragments through Biotinylated Random Primers; 5'PARE adaptor ligation to only those
182 containing 5-monophosphates; first-strand cDNA was generated from the ligated sequence
183 after reverse transcription using random hexamer 3' primer; a number of DNA products were
184 produced by PCR amplification. The library was single-end sequenced using an Illumina
185 Hiseq2500 platform at the LC-BIO (Hangzhou, China) following the vendor's recommended

186 protocol. CleaveLand 3.0 (Addo-Quaye *et al.*, 2009) was used for analysing sequencing data.
187 The raw data of degradome sequencing have been submitted to the NCBI GEO datasets under
188 the accession number SRP127561.

189 *Investigation of the target mRNAs of miRNAs by qRT-PCR*

190 Total RNA was extracted from the leaves with TRI Reagent (Sigma) according to the
191 manufacturer's instructions, and the samples were treated with DNase I enzyme (Promega).
192 Reverse transcription was performed using M-MLV Reverse Transcriptase and Oligo(dT) 15
193 primer (Promega) according to the manufacturer's instructions. The expression level of the
194 target genes was determined by real-time RT-PCR using recently planned primers (Table
195 S1A). The reactions were run on a CFX96 Real-Time PCR instrument (Bio-Rad) and the
196 relative fold change (FC) values were calculated according to (Boldizsár *et al.*, 2016).

197

198 *Computational prediction and analysis of miRNA targets*

199 The targets of the H₂O₂-induced miRNA collection were predicted with the psRNA Target
200 tool (<http://plantgrn.noble.org/psRNATarget/>). To confirm the degradome sequencing results
201 and to determine additional target genes the EnsemblPlants 31 release of wheat nucleotide
202 sequences were used as query cDNA library and the default scoring schema were used with
203 the following parameters: (1) # of top targets=200; (2) Penalty for G:U pair=0.5; (3) Extra
204 weight in seed region=1.5; (4) # of mismatch allowed in seed region=2; (5) Allow bulge
205 (gap) on target=enabled; (6) Penalty for opening gap=2; (7) Calculate target
206 accessibility=disabled; (8) Translation inhibition rate=10-11 NT; (9) Expectation=5; (10)
207 Penalty for other mismatches=1; (11) Seed region=2-13 NT; (12) HSP size=19; (13) Penalty
208 for extending gap=0.5.

209 MapMan (Thimm *et al.*, 2004) (<https://mapman.gabipd.org/>) and KEGG
210 (<http://www.genome.jp/kegg/>) pathway database were used for annotation of the miRNA
211 target genes. In addition, custom Blastx search was performed against the UniProt protein
212 database (<http://www.uniprot.org/downloads>) and the predicted miRNA targets using a
213 Geneious software version 9.8.1 (Biomatters, New Zealand; <http://www.geneious.com>).

214 The functional annotations were extended with gene expression data using an
215 oligonucleotide-based microarray (E-MTAB-6627:

216 <https://www.ebi.ac.uk/arrayexpress/experiments/E-MTAB-6627/>). Preparation of Cy5- and
217 Cy3-labelled cDNA using RNA isolated from the control and H₂O₂-treated samples,
218 respectively, and microarray hybridisation to a stress-specific 15k wheat oligonucleotide
219 microarray (Szűcs *et al.*, 2010) were performed as described (Szécsényi *et al.*, 2013). An
220 Agilent scanner (Agilent, Santa Clara, CA, USA) was employed for microarray scanning and
221 data collection as described previously (Kalapos *et al.*, 2016). The validation of microarray
222 was done by qRT-PCR as described for the target mRNAs of miRNAs and the primers are
223 listed in Table S1B.

224 The pathway map of the miRNAs and their target genes were build and visualized
225 using the yEd graph editor version 3.18.0.2 (yWorks, Germany;
226 <https://www.yworks.com/products/yed>).

227

228 *Statistical analysis*

229 Biochemical data from three independent experiments involving three biological repetitions
230 each were evaluated, and standard deviations are indicated in the figures. The statistical
231 analysis was prepared using one-way ANOVA and a least significant difference test or a
232 Dunnett T3 non-parametric test (if any condition had not been-fulfilled) (SPSS program). The
233 homogeneity of variances was tested by Levene's test. The relationships between the various
234 parameters were checked by correlation analysis (Excel program).

235

236 **Results**

237

238 *Growth parameters*

239 Treatment with H₂O₂ resulted in a transient wilting and rolling of the leaves after 1 h (Fig. 1).
240 After 2 h treatment the leaves of the treated plants recovered and were similar to the untreated
241 ones. However, the fresh and dry weight and the dry weight/ fresh weight ratio of the shoots
242 and roots were not affected by the H₂O₂ treatment (Fig. S1).

243

244 *Effect of H₂O₂ treatment on the non-enzymatic components of the AsA-GSH cycle*

245 Despite the visible effect of H₂O₂ on the plants after 1 h, there was no difference in H₂O₂
246 content between control and treated plants (Fig. 2). Subsequently a slight, gradual increase
247 was observed in the H₂O₂ content during the one-day long experiment in the leaves of both
248 untreated and H₂O₂-treated plants resulting in significant differences in certain sampling
249 points compared to the starting value.

250 The amount of DHA and the DHA/AsA ratio greatly decreased in the control and treated
251 leaves (to 50% or lower values compared to the starting value) while the amount of ASA and
252 the redox potential of the DHA/AsA redox couple did not change during the experiment
253 except for AsA in the control leaves after 24 h (Figs. 3A and 3B).

254 The concentration of GSH greatly increased after 3 h and remained nearly at this level until
255 the 6-hour sampling in control plants and decreased after 6 h in the leaves of the treated
256 seedlings compared to the starting value, which resulted in great differences between them
257 (Fig. 4A). After the H₂O₂ treatment, its minimum values were detected in the dark. The GSSG
258 concentration significantly increased at all sampling points under control conditions and after
259 3 h H₂O₂ treatment compared to the starting value. The GSSG/GSH ratio was greater both in
260 the control and treated seedlings than its initial value throughout the experiment. The half-cell
261 reduction potential of the GSSG/2GSH pair had a great increase after 6 h H₂O₂ treatment and
262 further on (Fig. 4B). In contrast to GSH, the amount and redox state of its precursor, cysteine
263 was not or only slightly affected by H₂O₂ (Fig. S2). The cysteine concentration was greater
264 only after 24 h in the control seedlings. The cystine content increased in untreated leaves and
265 remained unchanged in the treated ones except for the 3 h sampling compared to the starting
266 value. The cystine/cysteine ratio varied between 17.2 and 25.5% and the half-cell reduction
267 potential of this redox couple did not change during the whole experiment in both groups of
268 plants.

269

270 *Effect of H₂O₂ on the activity of antioxidant enzymes*

271 The activities of the antioxidant enzymes are given on a protein basis. Concentration of
272 protein did not change during the one-day experiment and was not affected by the H₂O₂
273 treatment (Fig. S3). The activity of CAT involved in the degradation of H₂O₂ increased both
274 in the control and treated seedlings during the experiment, and it returned to the starting value
275 after 24 h in the control seedlings, but remained high in the treated ones (Fig. 5A). However,
276 the activity of APX, removing H₂O₂ in the AsA-GSH cycle increased even after 1 h treatment
277 and was significantly greater compared to the starting value throughout the experiment while

278 such difference was observed for the control plants only after 3 and 12 h (Fig. 5B). The
279 activity of GR, which is also an enzymatic component of the AsA-GSH cycle like APX,
280 increased by 50% in both group of plants during the experiment and, after 24 h, it returned to
281 the initial value in the control seedlings but not in the treated ones (Fig. 5C). The activity of
282 GST, involved in the detoxification of xenobiotics and peroxides through catalysing their
283 conjugation with GSH, exhibited a similar tendency of changes as GR (Fig. 5D). However,
284 the increase in the activity in most sampling points (3, 6, 9, 12 h) compared to the starting
285 value and the difference between the control and treated seedlings after 24 h was greater,
286 about 2-fold.

287

288 *Determination of the H₂O₂-responsive miRNAs*

289 Small RNA sequencing was performed with samples collected after 0, 3 and 6 h treatment
290 repeated in 2 parallels, which means 6 sequencing in total. After removing the low-quality
291 and contaminant (length less than 18 nt or more than 30 nt reads) reads, 63.4 million reads
292 were obtained in total and among them 11.6 million were mapped as unique ones (Table S2).
293 The length distribution of the various small RNAs was similar in the different samples (Fig.
294 S4). The proportion of redundant reads was the highest (25%) for the 21 and 24 nt long
295 sequences and the proportion of unique sequences was the highest (60%) for the 24 nt long
296 sequences.

297 We determined the differential expression of known wheat miRNAs (Sun *et al.*, 2014)
298 between H₂O₂-treated and control seedlings. We found that a total of 70 miRNAs had a
299 minimum 1.5-fold difference between control and H₂O₂-treated seedlings and they formed 7
300 groups on the basis of the time-course of changes in their expression after 3 and 6 h treatment
301 compared to the starting value (Fig. 6). A transient increase was detected in the expression of
302 6 miRNAs after 3 h (group I), while the transcript level of 18 miRNAs (group V) remained
303 also high after 6 h. The expression of 7 miRNAs (group II) decreased transitionally after 3 h
304 and that of 6 miRNAs (group VII) was low after 6 h, too. Among the miRNAs the amount of
305 which exhibited no or slight changes during the first 3 hours of the treatment, the expression
306 of 21 (group III) and 10 (group IV) increased and decreased after 6 h, respectively.
307 Interestingly, the transcript level of 2 miRNAs (group VI) was lower after 3 h and higher after
308 6 h compared to the value detected before the H₂O₂ treatment.

309 The transcript levels of 8 H₂O₂-responsive miRNAs with a minimum 2-fold change in
310 their expression after 3 and/or 6 h compared to the starting value based on the sequencing
311 results (Table S3) were further checked in a time-course experiment with 7 sampling points
312 by qRT-PCR (Fig. 7). The tendency of H₂O₂-induced alterations obtained by the next
313 generation sequencing after 3 and 6 h treatment was confirmed by these measurements (for
314 tae-miR3106a and tae-miR3523a only in comparison with the starting value as done by the
315 sequencing) and tae-miR2007a, tae-miR3147a and tae-miR3523a were already induced after
316 1h H₂O₂ treatment. Without treatment, the expression of the selected miRNAs exhibited a
317 daily pattern: in several cases with higher levels during the light period and lower ones during
318 the night (Figs. 7A, 7C, 7F and 7H). This pattern was modified by the H₂O₂ treatment. The
319 miRNAs' levels were at least 2-fold greater after 24 h H₂O₂ treatment compared to the control
320 values except for miR3106a having a 50% decrease in its expression. For tae-miR2007a, tae-
321 miR818h and tae-miR3074a this difference was 9-fold or greater. The miRNA levels were
322 minimum 4-fold greater for miR3106a after 3 h and 12 h and for miR3074a after 1 h in
323 control seedlings compared to the treated ones in the same sampling point.

324

325 *Identification of the target genes of the H₂O₂-responsive miRNAs*

326 In order to determine those target genes of the H₂O₂-responsive miRNAs whose products are
327 cleaved in our experimental system, RNAs obtained from samples taken after 0h, 3h and 6h
328 H₂O₂ treatment were mixed equally for degradome sequencing. In this analysis 13.5 million
329 raw reads were obtained and after the data analysis 160,466 covered cDNA sequences could
330 be identified (Table S3). Based on the degradome sequencing, 86 unique target sequences of
331 28 H₂O₂-responsive miRNAs could be identified. For 29 target genes, the H₂O₂-
332 responsiveness was also shown by microarray analysis (validated by qRT-PCR, r²: 0.68, Fig.
333 S5) and these genes are related to transcription, redox regulation, protein phosphorylation and
334 degradation (Table S3). Two targets of tae-miR3493b, the genes encoding peroxidase 52 and
335 a thioredoxin-like protein, and one target of tae-miR3513a encoding thioredoxin H8 are
336 components of the antioxidant system. Both miRNAs were induced by H₂O₂ (Fig. 6, group
337 III) and the expression of their targets were repressed as shown by microarray analysis (Table
338 S3).

339 The time-course of changes in the expression of target genes of those 8 H₂O₂-
340 responsive miRNAs shown in Fig. 7 was also investigated. Similarly, to the corresponding

341 miRNAs, the expression of their targets genes also exhibited a daily rhythm in the untreated
342 seedlings, which was altered by H₂O₂. For several targets the direction of changes was
343 opposite in the control and treated plants, which resulted in great differences between the
344 transcript levels in certain sampling points (Figs. 8A, 8C, 8D, 8H). The expressions were
345 influenced by the treatment already in the first 3 h and the difference between the control and
346 treated seedlings was minimum 2-, but sometimes 10-fold at least in one sampling point for
347 all target genes. Five of the targets were already induced after 1 or 3 h treatment (Figs. 8B,
348 8C, 8F, 8G and 8H), one only after 24 h (Fig. 8E) and two of them were repressed (Figs. 8A
349 and 8D). A moderate negative correlation (r: -0.38 – -0.42) between the expression of the
350 following miRNA and target pairs was found after H₂O₂ treatment: tae-miR2007A – ribulose-
351 1.5-bisphosphate carboxylase activase, tae-miR3106 – beta-carotene isomerase, tae-
352 miR3523a – glycerol-3-phosphate dehydrogenase. For 3 pairs a low negative correlation and
353 for 2 pairs low positive correlation was observed.

354 Using bioinformatics tools 6808 unique target sequences (from them 86 were
355 identified by degradome sequencing) of 70 H₂O₂-responsive miRNAs were found (Table S3).
356 The following targets were related to the components of the AsA-GSH system or other
357 antioxidants: tae-miR3369a – a phosphomannomutase involved in AsA biosynthesis, tae-
358 miR3513a– monodehydroascorbate reductase, tae-miR3506b– peroxidase, tae-miR506b –
359 GST, tae-miR3064a, tae-miR3510a, – thioredoxin. For 1647 targets the H₂O₂-responsiveness
360 was also demonstrated by microarray study (Table S3).

361 Based on their targets, two types of KEGG-analysis of H₂O₂-responsive miRNAs were
362 prepared using the database available for *Brachypodium*, a closely relative species to wheat
363 (Table S5, Fig. S6). In the first one, the number of H₂O₂-responsive miRNAs was compared
364 to the total number of the miRNAs in the individual categories in which the miRNAs were
365 grouped based on their targets. The greatest number of such miRNAs was related to ‘plant-
366 pathogen interaction (bdi04626)’, ‘protein processing in endoplasmatic reticulum
367 (bdi04141)’, ‘carbon metabolism (bdi01200)’, ‘biosynthesis of amino acids (bdi01230)’,
368 ‘purine metabolism (bdi00230)’, processes in ‘spliceosome (bdi03040)’ and ‘plant hormone
369 signal transduction (bdi04075)’ (Fig. S6). In the second approach, the number of H₂O₂-
370 responsive target genes was analysed. The two analyses gave different results since one
371 miRNA may have several target genes and one target gene may be controlled by several
372 miRNAs.

373 While the abundance of the H₂O₂-responsive miRNA in relation to the whole miRNA
374 set in wheat was maximum 10% in the various KEGG-pathway categories (first evaluation
375 approach), this ratio was at least 30% for 45% of target genes (second approach, Fig. S6).
376 Taking into account the 7 greatest groups of categories, the same ones were selected by both
377 approaches except for the ‘purine metabolism (bdi00230)’ by grouping of miRNAs and
378 ‘ribosome-related processes (bdi03010)’ by grouping of targets. The enrichment of targets of
379 H₂O₂-responsive miRNAs in the categories related to AsA and GSH metabolism, peroxisome,
380 proteasome varied between 20-35%.

381 The possible interactions of the identified 70 H₂O₂-responsive miRNAs with their
382 6808 targets were also analysed (Fig. S7). This network with 9620 connections shows that
383 most miRNAs have several targets, and most of the targets are controlled only by one
384 miRNAs. However, several of them are regulated by two or more miRNAs therefore the
385 miRNAs and their targets form a complex network.

386 In the central part of this network are located tae-miR818b, tae-miR818c, tae-
387 miR818m, tae-miR818k, tae-miR818h, tae-miR3369a, tae-miR3523a and tae-miR3506b (Fig.
388 9) having 233 targets with 1437 connections. In this part of the network tae-miR3369a and
389 members of the tae-miR818 family control the expression of many genes at translational
390 level, while tae-miR3506b and tae-miR3523a does so by cleavage of their target mRNAs
391 (Table S3). Most targets of these 8 miRNAs are involved in transcriptional regulation, protein
392 phosphorylation and degradation (Table S6A). Based on KEGG categories, they were mainly
393 (3-8 targets/ category) related to the processes in spliceosome, biosynthesis of amino acids,
394 protein processing in ER, carbon, purine, starch and sucrose metabolism (Table S6B). Using a
395 microarray analysis, the level and direction of the expression changes of several (1647) H₂O₂-
396 responsive target genes were also determined (Table S3). From the targets of tae-miR3369a,
397 25 were present on the array and among them the expression of 12 and 6 genes increased and
398 decreased, respectively. It is worth mention that for miR3493b, 16 of the 35 targets and for
399 miR156a, 4 of the 17 targets were also identified by degradome sequencing.

400

401 **Discussion**

402

403 *Effect of H₂O₂ on the redox environment in the leaves*

404 Induction of oxidative stress is a common consequence of abiotic stresses. This effect was
405 successfully simulated by H₂O₂ treatment previously in wheat and maize as shown by the
406 modification of the redox environment (Kellős *et al.*, 2008; Gulyás *et al.*, 2014). Although the
407 effect of H₂O₂ on the miRNA profile was investigated in rice and *Brachypodium*, the possible
408 involvement of the AsA-GSH cycle and other antioxidants in the control of miRNA levels
409 was not studied in these experiments (Li *et al.*, 2011; Lv *et al.*, 2016). In the present
410 experimental system, H₂O₂ treatment efficiently modified the GSH-dependent redox
411 environment and activated the related protective mechanisms in the leaves of wheat seedlings
412 therefor the growth was not affected as shown by fresh and dry weight data. The H₂O₂-
413 induced transient wilting and rolling of the leaves, as a part of the protection, may be due to a
414 rapid loss of water content by the opening of stomata induced by transient local changes in
415 H₂O₂ concentration since H₂O₂ signaling is involved in the control of stomatal movement
416 (Hua *et al.*, 2012). The alterations in the GSH-dependent redox environment are indicated by
417 the decrease in GSH content and increase in E_{GSSG/2GSH} value compared to the untreated
418 control plants. After a 3 h treatment when the first sampling for miRNA sequencing was
419 prepared, the GSH content was by 30% lower in the treated seedlings than in the controls. In
420 contrast to GSH, the AsA concentration and E_{DHA/AsA} value did not change which can be
421 explained by the 3 times greater size of the AsA pool compared to the GSH pool. APX,
422 having an increased activity throughout the H₂O₂ treatment could successfully decompose the
423 unnecessary H₂O₂ in plants deriving from its addition to the nutrient solution. Thus, no change
424 in the endogenous H₂O₂ concentration was detected in leaf tissue extracts which does not
425 exclude the local changes in its level in specific cells (stomata) and organelles (chloroplasts).
426 However, during the removal of H₂O₂ in the AsA-GSH cycle, the amount and redox state of
427 GSH also changed in leaf extracts because of its oxidation by GR having increased activity
428 after 24 h treatment. In addition, the larger use of GSH by GST after 24 h for the
429 detoxification of peroxides in the H₂O₂-treated plants will also reduce the GSH concentration.
430 Besides, APX, CAT also could greatly contribute to the degradation of H₂O₂ since its activity
431 was greater by 60% after 24 h in the treated seedlings compared to the control ones. The
432 correlations between the expression levels of miRNAs, their target mRNAs and antioxidants
433 (GSH, APX, GST, CAT) in the treated seedlings show the closeness and direction of their
434 relationships (Table S7), The control of miRNAs by GSH was corroborated for miR395 in S-
435 deprived *Arabidopsis*, since the expression of this miRNA was modified after addition of
436 exogenous GSH or in GSH-deficient mutants (Jagadeeswaran *et al.*, 2014). In addition, tae-
437 miR395 was H₂O₂-responsive in wheat (present study) and in *Brachypodium* (Lv *et al.*, 2016).

438 These results indicate that the effect of H₂O₂ on miRNAs is mediated by certain components
439 of the AsA-GSH cycle, which has a central role in the redox regulation (Foyer and Noctor,
440 2011).

441

442

443 *Effect of H₂O₂ on miRNA profiles*

444 The H₂O₂-induced modification of the GSH-dependent redox environment had a great effect
445 on the miRNA profile since a minimum 1.5-fold change was shown by the sequencing results
446 in the expression of 70 miRNAs. Far more miRNAs were upregulated (44) than
447 downregulated (22). Furthermore, some of them (4) was inhibited first (after 3 h) and induced
448 afterwards (after the subsequent 3 h) in wheat. Similarly to wheat, a large number of miRNAs
449 (61) was affected by H₂O₂ in *Brachypodium* (Lv *et al.*, 2016) while only 7 in rice (Li *et al.*,
450 2011). The low number of H₂O₂-responsive miRNAs in rice is surprising, since the
451 developmental stage of seedlings (2-3 leaves), the applied concentration of H₂O₂ (10-20 mM)
452 and the duration of treatment (2-6 h) were similar in all 3 species. These results indicate the
453 greater sensitivity of the miRNA-related regulatory system to oxidative stress in the
454 phylogenetically nearer wheat and *Brachypodium* compared to the more distant rice.

455 The ratio of H₂O₂-responsive miRNAs compared to their total number was very similar
456 (mainly 1:10) within the various KEGG-categories in wheat. Among the categories with the
457 greatest number of H₂O₂-responsive miRNAs were carbon metabolism, peroxisome-
458 associated reactions including the glyoxylate pathway. These processes are related to the
459 chloroplasts and peroxisomes (Slesak *et al.*, 2007), the major organelles responsible for the
460 production of H₂O₂ explaining the large number of H₂O₂-responsive miRNAs in the
461 metabolic pathways occurring in these organelles. Besides the H₂O₂ formation, peroxisome
462 and chloroplast are also connected to the redox system through the formation of glycine and
463 γ -glutamylcysteine, respectively, since these compounds are precursors of GSH. Two other
464 main KEGG-categories with high number of H₂O₂-responsive miRNAs were the 'protein
465 processing in the endoplasmatic reticulum (bdi04141)' and the 'proteasome-related
466 degradation of proteins (bdi03020)'. The endoplasmatic reticulum is the main source of H₂O₂
467 in the cytosol (Slesak *et al.*, 2007), and proteasomes are protein complexes where H₂O₂-
468 mediated S-glutathionylation of proteins takes place if the cellular redox state shifts (Jung *et*

469 *al.*, 2014). In this process the H₂O₂-dependent alteration in the ratio of GSH/GSSG may affect
470 the metabolism of proteins by the involvement of miRNAs.

471 Although several H₂O₂-responsive miRNAs were found in wheat (total H₂O₂-
472 responsive: 70) and *Brachypodium* (total H₂O₂-responsive: 61) (Lv *et al.*, 2016), only two of
473 them, tae-miR160b and tae-miR395a were common between the two plant species (Table S8).
474 Tae-miR395a is involved in sulphate reduction and therefore indirectly in the GSH formation
475 through cysteine; tae-miR160b has auxin-related function. Thus, the basic regulatory
476 processes such as hormonal and redox regulations are conserved between these two species.
477 While no overlap of H₂O₂-responsive miRNAs was observed between wheat and rice,
478 miR169d, miR827-3p, miR397a and miR408-5p were affected by H₂O₂ both in
479 *Brachypodium* and rice (total H₂O₂-responsive: 7) (Li *et al.*, 2011; Lv *et al.*, 2016). They
480 regulate the genes encoding HAP2-like transcription factor, SPX-domain protein (regulation
481 of phosphate homeostasis), laccase (lignin biosynthesis) and a monosaccharide transport
482 protein, respectively. The limited overlap in H₂O₂-related miRNAs between the three species
483 indicates the specificity of the miRNAs in the various organisms during the response to
484 environmental changes.

485 Similarly, to H₂O₂ in wheat, ozone-induced oxidative stress also affected the members
486 of the miR156 family (controlling flowering, yield and leaf initiation) in *Arabidopsis* (Table
487 S8) (Iyer *et al.*, 2012). However, the members of the other 21 ozone-responsive miRNAs
488 family were not influenced by H₂O₂ in wheat. Between rice and *Arabidopsis*, also only one
489 common oxidative stress-responsive miRNA family, the miR169 (target: HAP2-like
490 transcription factor), exists, which is involved in the stress-response (Li *et al.*, 2011; Iyer *et*
491 *al.*, 2012). Members of miR169 family were also induced by H₂O₂ in *Brachypodium* (Lv *et*
492 *al.*, 2016). In addition, miR160a (target: auxin response factor 22) and miR164 (target:
493 phytoene dehydrogenase) were induced both in *Arabidopsis* and in *Brachypodium* by
494 oxidative stress. These experiments indicate that different sets of miRNAs are involved in the
495 response to various oxidants such as H₂O₂ and O₃. In addition, the response of the members of
496 the same miRNA family to the various abiotic stresses in generally also differs in the different
497 plant species. However, some similarities can also be found when comparing the miRNA set
498 induced by oxidative and various abiotic stresses in *Arabidopsis* (Zhang, 2015; Barciszewska-
499 Pacak *et al.*, 2015). Therefore, it is difficult to describe the involvement of the individual
500 miRNAs in the stress response with a general model. The differences between the plant

501 species may be due to the complex regulatory networks of miRNAs in which the role of the
502 individual miRNAs varies between the species.

503 When checking the effect of H₂O₂ on miRNAs by qRT-PCR in a time course
504 experiment during 1 day, light-dependent daily changes were observed in their levels even in
505 the untreated seedlings, which observation corresponds with the light-responsiveness of
506 miRNAs demonstrated in *Brassica rapa* (Zhou *et al.*, 2016). A redox control of these light-
507 dependent daily alterations can be supposed since it was modified by H₂O₂ in wheat. The
508 tendency of changes in the expression of the miRNAs detected by sequencing after 3 and 6 h
509 treatment with H₂O₂ could be confirmed by qRT-PCR. After 9, 12 and 24 h exposure to H₂O₂,
510 the expression of those miRNAs also differed very often that were grouped together based on
511 the initial changes after 3 and 6 h H₂O₂ treatment in their transcription. Only some miRNAs
512 with an increase after 6 h H₂O₂ treatment (tae-miR3147a, tae-miR3074a) exhibited similar
513 time-course of expression changes after 9, 12 and 24 h of H₂O₂ addition. The observed large
514 increase in the expression of these 2 miRNAs during the first 6 h was probably due to the
515 additive effect of H₂O₂ and light, since the transcript levels became far lower in the dark even
516 after 1 h. In contrast, the amount of tae-mir3106a still remained high after 1 h in the dark and
517 it decreased only after 4 h in the treated plants. The effect of light on H₂O₂-responsive
518 miRNAs is further supported by the fact that the expression of 5 of them increased again in
519 the light after the transient decrease in the dark during the 1-day H₂O₂ treatment.

520

521 *Function of the selected miRNAs based on their target genes*

522 By bioinformatics tools we could identify 6808 possible targets for the 70 identified H₂O₂-
523 responsive miRNAs. However, by degradome sequencing only 86 targets of 28 of them could
524 be determined indicating that only this small set is actually affected by miRNAs after 0, 3 or 6
525 h in our experimental system. This large difference could derive from the possible temporal
526 and spatial shift in the expression changes in miRNAs and their targets and the existence of
527 complex regulatory network including opposite miRNA regulators of the same target
528 (Kawashima *et al.*, 2009; Liang *et al.*, 2014). Thus, a temporal shift in the expression was
529 found for tae-miR3106 and its target, beta-carotene isomerase. Among the target genes
530 determined by degradome sequencing several were related to transcriptional regulation
531 (targets of tae-miR156a, tae-miR3294b, tae-miR3369a, tae-miR3493aa), protein
532 phosphorylation (targets of tae-miR3319b, tae-miR3332a), protein degradation (targets of tae-

533 miR3369a, tae-miR818b, tae-miR2001a, tae-miR399b), and redox regulation (targets of tae-
534 miR3493a, tae-miR3513a) and the core part of our regulatory network model was also
535 associated with these processes. The H₂O₂ responsiveness of these target genes was also
536 confirmed by microarray analysis in wheat. In addition, the KEGG analysis confirmed the
537 enrichment of the target genes of H₂O₂-responsive miRNAs in the categories related to
538 protein metabolism and redox processes. Although the degradation of few target mRNAs was
539 only checked in *Brachypodium* and rice (Li *et al.*, 2011; Lv *et al.*, 2016), the effect of H₂O₂
540 was shown for several redox- and protein decomposition-related proteins in these species, too
541 (Wan and Liu, 2008; Bian *et al.*, 2015). These results are in accordance with those ones
542 obtained in wheat with degradome analysis because of the occurrence of common functional
543 categories such as redox regulation and protein degradation.

544 The present results indicate a feed-back regulation between the redox system and the
545 miRNAs since the H₂O₂-induced modification of GSH level and APX activity affected
546 several miRNAs the target of which control the levels of redox compounds in wheat (Fig. 10).
547 Thus, by degradome sequencing, three miRNAs (tae-miR3493b – target genes: peroxidase 52
548 and a thioredoxin-like protein; tae-miR3513a – target gene: thioredoxin H8) and by
549 bioinformatics tools, 6 miRNAs were found. This hypothesis was also corroborated in the
550 case of miR395 controlling the synthesis of the GSH precursor, cysteine. It also proved to be
551 H₂O₂-responsive in *Brachypodium* (Lv *et al.*, 2016) and its expression depended on the
552 availability of GSH in *Arabidopsis* (Jagadeeswaran *et al.*, 2014). Besides the indirect control
553 of miRNAs through various antioxidants, H₂O₂ may also directly affect miRNAs as it was
554 suggested for heavy metals (Min Yang and Chen, 2013). Instead of linear relationships, a
555 network of mutual interactions can be supposed among H₂O₂, other redox compounds,
556 miRNAs and metabolism which allows a continuous redox-dependent adjustment of miRNA
557 levels and the related metabolic processes (Fig. 10).

558 Although the first 6 h were very important in the response of miRNAs and their targets
559 to H₂O₂ in wheat, *Brachypodium* and rice (Li *et al.*, 2011; Lv *et al.*, 2016), the subsequent
560 changes are also determinative for the reaction to stress as it was observed in wheat for 8
561 miRNAs and their targets during a whole day time-course experiment. Similarly, to the 8
562 miRNAs selected for qRT-PCR, their target genes also exhibited a light-dependent daily
563 rhythm in untreated seedlings. This observation is not surprising since the light intensity
564 changes during the day, which affects the possible formation of ROS in the photosynthetic
565 electron transport chain and subsequently the redox-sensitive miRNAs and their targets will

566 be influenced. In our experimental approach we could detect these light-responsive miRNAs
567 and their targets probably by modifying the amount of ROS after the addition of H₂O₂ to the
568 nutrient solution of the plants.

569 Although, for certain miRNA-target pairs, we observed the expected negative
570 correlation, it was not detected for each of them. The lack of such relationship can be
571 explained by the function of miRNAs as mobile signalling elements during the H₂O₂-
572 dependent regulation of gene expression for which a model was recently established in
573 *Arabidopsis* (Liang *et al.*, 2014). Based on this model miRNA can act in another cell, tissue or
574 organ on their target genes. Consistent with this hypothesis, in the case of miR395 and its
575 target involved in the sulphur assimilation, a positive temporal but negative spatial correlation
576 was found in *Arabidopsis* (Kawashima *et al.*, 2009). Besides the mentioned dynamic changes
577 in miRNA levels, such alteration also occurs in ROS levels because of the
578 compartmentalisation of ROS production and removal (Noctor *et al.*, 2018) that allows even a
579 more complex redox-dependent regulation of miRNA targets.

580 A further possible explanation for the lack of the expected negative correlation between
581 the level of the miRNAs and their targets is the existence of such regulatory networks in
582 which one target genes is regulated by several miRNAs, and one miRNA controls several
583 targets in wheat. In addition, a positive post-transcriptional regulation of gene expression is
584 also possible as described recently for miR171b controlling arbuscular mycorrhizal symbiosis
585 in *Medicago trunculata* (Couzigou *et al.*, 2017). Thus, in our network the result of the
586 negative and positive regulatory effects could be a very fine regulation with small changes. In
587 this network tae-miR33506b, tae-miR3523a, tae-miR3369a and members of the tae-miR818
588 family have central position with many target through which they are interconnected with
589 other miRNAs. Similar regulatory network of H₂O₂-responsive miRNAs and their targets was
590 also proposed in *Brachypodium* in which also a large number of target genes is controlled by
591 one miRNA (Lv *et al.*, 2016). This system allows a co-ordinated regulation of a large set of
592 genes. Probably only a small part of the many possible targets of a miRNA is regulated in a
593 certain time point depending on the organ, developmental stage, environmental effects and
594 regulatory interactions of various signalling pathways as indicated by the large difference in
595 the number of the targets detected by degradome sequencing and predicted by bioinformatics
596 tools in wheat All small RNA libraries prepared for this study were sequenced with Illumina
597 Hiseq 2000.

598

599 *Conclusions*

600 H₂O₂ can modify the redox state in wheat through its effect on GSH, APX and other
601 antioxidants which in turn influence the expression of miRNAs and their target genes and
602 subsequently the metabolism. A network of interactions between the components of this
603 model can be proposed. From the 70 H₂O₂-responsive miRNAs, for 28 miRNAs 86 target
604 genes were identified and these genes are related to transcriptional regulation, protein
605 phosphorylation, protein degradation and redox regulation as shown by degradome analysis.
606 Based on a bioinformatics analysis, a regulatory network of 70 miRNAs with 6808 unique
607 targets was created, which enables the fine adjustment a large set of redox-responsive genes.

608

609 **Supplementary data**

610 Supplementary data are available at JXB online.

611 **Fig. S1.** Effect of H₂O₂ treatment on the fresh and dry weight and dry to fresh weight ratio of
612 shoots and roots.

613 **Fig. S2.** Effect of H₂O₂ treatment on the size and redox state of the cysteine pool.

614 **Fig. S3.** Effect of H₂O₂ treatment on the protein content.

615 **Fig. S4.** Proportion of redundant and unique reads in miRNA transcriptome.

616 **Fig. S5.** Regression analysis of gene expression results obtained by microarray and qRT-PCR.

617 **Fig. S6.** KEGG-analysis of H₂O₂-responsive miRNAs and their targets.

618 **Fig. S7.** The whole network of the H₂O₂-responsive miRNAs and their targets determined by
619 degradome sequencing and bioinformatics tools.

620 **Table S1.** Primers used for the qRT-PCR analysis of miRNAs target genes and validation of
621 microarray data.

622 **Table S2.** Results of small RNA sequencing.

623 **Table S3.** H₂O₂-responsive miRNAs and their target genes

624 **Table S4.** Summary of degradome sequencing.

625 **Table S5.** KEGG categories of the targets of H₂O₂-responsive miRNAs.

626 **Table S6.** Correlations between the time-course of changes during 1-day H₂O₂ treatments in
627 the level of antioxidants, selected miRNAs and their target mRNAs investigated by qRT-
628 PCR.

629 **Table S7.** Genes and their regulator miRNAs in the core network (A) and distribution of core
630 network (Fig. 9) miRNAs and their target genes in different KEGG metabolic pathways (B).

631 **Table S8.** miRNAs responsive to oxidative stress in two or more species.

632

633

634 **Acknowledgements**

635 The authors thank Apollónia Horváth and Mónika Fehér for their help in plant cultivation and
636 treatment and Csilla Terézia Nagy and Mohamed Ahres for the biochemical measurements.
637 This work was funded by the National Research, Development and Innovation Office
638 (Hungary, grant IDs: TÉT_12_CN-1-2012-0002 and ANN 117949) and the National Key
639 Research and Development Program of China (2016YFD0101004).

References

- Addo-Quaye C, Miller W, Axtell MJ.** 2009. CleaveLand: a pipeline for using degradome data to find cleaved small RNA targets. *Bioinformatics* **25**, 130–131.
- Audic S, Claverie J-M.** 1997. The Significance of Digital Gene Expression Profiles. *Genome Research* **7**, 986–995.
- Barciszewska-Pacak M, Milanowska K, Knop K, et al.** 2015. *Arabidopsis* microRNA expression regulation in a wide range of abiotic stress responses. *Frontiers in Plant Science* **6**, 410.
- Bian Y-W, Lv D-W, Cheng Z-W, Gu A-Q, Cao H, Yan Y-M.** 2015. Integrative proteome analysis of *Brachypodium distachyon* roots and leaves reveals a synergetic responsive network under H₂O₂ stress. *Journal of Proteomics* **128**, 388–402.
- Boldizsár Á, Vanková R, Novák A, Kalapos B, Gulyás Z, Pál M, Floková K, Janda T, Galiba G, Kocsy G.** 2016. The *mvp2* mutation affects the generative transition through the modification of transcriptome pattern, salicylic acid and cytokinin metabolism in *Triticum monococcum*. *Journal of Plant Physiology* **202**, 21–33.
- Bradford MM.** 1976. A rapid and sensitive method for the quantitation of microgram quantities of protein utilizing the principle of protein-dye binding. *Analytical Biochemistry* **72**, 248–254.
- Considine MJ, Foyer CH.** 2014. Redox regulation of plant development. *Antioxidants & redox signaling* **21**, 1305–26.
- Couzigou J-M, Laressergues D, André O, Gutjahr C, Guillotin B, Bécard G, Combier J-P.** 2017. Positive Gene Regulation by a Natural Protective miRNA Enables Arbuscular Mycorrhizal Symbiosis. *Cell Host & Microbe* **21**, 106–112.
- Desikan R, A.-H.-Mackerness S, Hancock JT, Neill SJ.** 2001. Regulation of the *Arabidopsis* Transcriptome by Oxidative Stress. *Plant Physiology* **127**, 159–172.
- Dryanova A, Zakharov A, Gulick PJ.** 2008. Data mining for miRNAs and their targets in the Triticeae (G Scoles, Ed.). *Genome* **51**, 433–443.
- Foyer CH, Lopez-Delgado H, Dat JF, Scott IM.** 1997. Hydrogen peroxide- and glutathione-

associated mechanisms of acclimatory stress tolerance and signalling. *Physiologia Plantarum* **100**, 241–254.

Foyer CH, Noctor G. 2011. Ascorbate and glutathione: the heart of the redox hub. *Plant physiology* **155**, 2–18.

Griffiths-Jones S. 2004. Rfam: annotating non-coding RNAs in complete genomes. *Nucleic Acids Research* **33**, D121–D124.

Griffiths-Jones S, Bateman A, Marshall M, Khanna A, Eddy SR. 2003. Rfam: an RNA family database. *Nucleic Acids Research* **31**, 439–441.

Gulyás Z, Boldizsár Á, Novák A, Szalai G, Pál M, Galiba G, Kocsy G. 2014. Central role of the flowering repressor *ZCCT2* in the redox control of freezing tolerance and the initial development of flower primordia in wheat. *BMC Plant Biology* **14**, 91.

Hossain MA, Bhattacharjee S, Armin S-M, Qian P, Xin W, Li H-Y, Burritt DJ, Fujita M, Tran L-SP. 2015. Hydrogen peroxide priming modulates abiotic oxidative stress tolerance: insights from ROS detoxification and scavenging. *Frontiers in Plant Science* **6**, 420.

Hua D, Wang C, He J, Liao H, Duan Y, Zhu Z, Guo Y, Chen Z, Gong Z. 2012. A Plasma Membrane Receptor Kinase, GHR1, Mediates Abscisic Acid- and Hydrogen Peroxide-Regulated Stomatal Movement in *Arabidopsis*. *The Plant Cell* **24**, 2546–2561.

Iyer NJ, Jia X, Sunkar R, Tang G, Mahalingam R. 2012. microRNAs responsive to ozone-induced oxidative stress in *Arabidopsis thaliana*. *Plant Signaling and Behavior* **7**, 484–491.

Jagadeeswaran G, Li YF, Sunkar R. 2014. Redox signaling mediates the expression of a sulfate-deprivation-inducible microRNA395 in *Arabidopsis*. *Plant Journal* **77**, 85–96.

Jung T, Höhn A, Grune T. 2014. The proteasome and the degradation of oxidized proteins: Part II – protein oxidation and proteasomal degradation. *Redox Biology* **2**, 99–104.

Kalapos B, Dobrev P, Nagy T, Vítámvás P, Györgyey J, Kocsy G, Marincs F, Galiba G. 2016. Transcript and hormone analyses reveal the involvement of ABA-signalling, hormone crosstalk and genotype-specific biological processes in cold-shock response in wheat. *Plant Science* **253**, 86–97.

Kawashima CG, Yoshimoto N, Maruyama-Nakashita A, Tsuchiya YN, Saito K,

- Takahashi H, Dalmay T.** 2009. Sulphur starvation induces the expression of microRNA-395 and one of its target genes but in different cell types. *The Plant Journal* **57**, 313–321.
- Kellős T, Timár I, Szilágyi V, Szalai G, Galiba G, Kocsy G.** 2008. Stress hormones and abiotic stresses have different effects on antioxidants in maize lines with different sensitivity. *Plant Biology* **10**, 563–572.
- Khraiwesh B, Zhu J-K, Zhu J.** 2012. Role of miRNAs and siRNAs in biotic and abiotic stress responses of plants. *Biochimica et Biophysica Acta* **1819**, 137–148.
- Kidner CA, Martienssen RA.** 2005. The developmental role of microRNA in plants. *Current Opinion in Plant Biology* **8**, 38–44.
- Kocsy G, Szalai G, Vágújfalvi A, Stéhli L, Orosz G, Galiba G.** 2000. Genetic study of glutathione accumulation during cold hardening in wheat. *Planta* **210**, 295–301.
- Kocsy G, Tari I, Vanková R, Zechmann B, Gulyás Z, Poór P, Galiba G.** 2013. Redox control of plant growth and development. *Plant science : an international journal of experimental plant biology* **211**, 77–91.
- Kranner I, Grill D.** 1996. Determination of Glutathione and Glutathione Disulphide in Lichens: a Comparison of Frequently Used Methods. *Phytochemical Analysis* **7**, 24–28.
- Langmead B, Salzberg SL.** 2012. Fast gapped-read alignment with Bowtie 2. *Nature Methods* **9**, 357–359.
- Li T, Li H, Zhang YX, Liu JY.** 2011. Identification and analysis of seven H₂O₂-responsive miRNAs and 32 new miRNAs in the seedlings of rice (*Oryza sativa* L. ssp. *indica*). *Nucleic Acids Research* **39**, 2821–2833.
- Liang D, White RG, Waterhouse PM.** 2014. Mobile gene silencing in *Arabidopsis* is regulated by hydrogen peroxide. *PeerJ* **2**, e701.
- Locato V, Cimini S, De Gara L.** 2018. ROS and redox balance as multifaceted players of cross-tolerance: epigenetic and retrograde control of gene expression. *Journal of Experimental Botany* **69**, 3373–3391.
- Lv D-W, Zhen S, Zhu G-R, Bian Y-W, Chen G-X, Han C-X, Yu Z-T, Yan Y-M.** 2016. High-Throughput Sequencing Reveals H₂O₂ Stress-Associated MicroRNAs and a Potential

Regulatory Network in *Brachypodium distachyon* Seedlings. *Frontiers in Plant Science* **7**, 1–20.

Martin M. 2011. Cutadapt removes adapter sequences from high-throughput sequencing reads. *EMBnet.journal* **17**, 10–12.

Min Yang Z, Chen J. 2013. A potential role of microRNAs in plant response to metal toxicity. *Metallomics* **5**, 1184.

Nawrocki EP, Burge SW, Bateman A, et al. 2015. Rfam 12.0: updates to the RNA families database. *Nucleic Acids Research* **43**, D130–D137.

Neill SJ, Desikan R, Clarke A, Hurst RD, Hancock JT. 2002. Hydrogen peroxide and nitric oxide as signalling molecules in plants. *Journal of Experimental Botany* **53**, 1237–1247.

Noctor G, Mhamdi A, Foyer CH. 2016. Oxidative stress and antioxidative systems: recipes for successful data collection and interpretation. *Plant, Cell & Environment* **39**, 1140–1160.

Noctor G, Reichheld J-P, Foyer CH. 2018. ROS-related redox regulation and signaling in plants. *Seminars in Cell & Developmental Biology* **80**, 3–12.

Phillips JR, Dalmay T, Bartels D. 2007. The role of small RNAs in abiotic stress. *FEBS Letters* **581**, 3592–3597.

Rajwanshi R, Chakraborty S, Jayanandi K, Deb B, Lightfoot DA. 2014. Orthologous plant microRNAs: microregulators with great potential for improving stress tolerance in plants. *Theoretical and Applied Genetics* **127**, 2525–2543.

Roach T, Stögl W, Baur T, Kranner I. 2018. Distress and eustress of reactive electrophiles and relevance to light stress acclimation via stimulation of thiol/disulphide-based redox defences. *Free Radical Biology and Medicine* **122**, 65–73.

Rubio-Somoza I, Weigel D. 2011. MicroRNA networks and developmental plasticity in plants. *Trends in Plant Science* **16**, 258–264.

Schafer FQ, Buettner GR. 2001. Redox environment of the cell as viewed through the redox state of the glutathione disulfide/glutathione couple. *Free Radical Biology & Medicine* **30**, 1191–1212.

Slesak I, Libik M, Karpinska B, Karpinski S, Miszalski Z. 2007. The role of hydrogen

peroxide in regulation of plant metabolism and cellular signalling in response to environmental stresses. *Acta Biochim Polonica* **54**, 39–50.

Soltész A, Tímár I, Vashegyi I, Tóth B, Kellós T, Szalai G, Vágújfalvi A, Kocsy G, Galiba G. 2011. Redox changes during cold acclimation affect freezing tolerance but not the vegetative/reproductive transition of the shoot apex in wheat. *Plant Biology* **13**, 757–766.

Sun F, Guo G, Du J, Guo W, Peng H, Ni Z, Sun Q, Yao Y. 2014. Whole-genome discovery of miRNAs and their targets in wheat (*Triticum aestivum* L.). *BMC Plant Biology* **14**, 142.

Szalai G, Janda T, Pál M. 2014. Routine sample preparation and HPLC analysis for ascorbic acid (vitamin C) determination in wheat plants and *Arabidopsis* leaf tissues. *Acta Biologica Hungarica* **65**, 205–217.

Szécsényi M, Cserhádi M, Zvara Á, Dudits D, Györgyey J. 2013. Monitoring of transcriptional responses in roots of six wheat cultivars during mild drought stress. *Cereal Research Communications* **41**, 527–538.

Szűcs A, Jäger K, Jurca ME, Fábrián A, Bottka S, Zvara Á, Barnabás B, Fehér A. 2010. Histological and microarray analysis of the direct effect of water shortage alone or combined with heat on early grain development in wheat (*Triticum aestivum*). *Physiologia Plantarum* **140**, 174–188.

Thimm O, Bläsing O, Gibon Y, Nagel A, Meyer S, Krüger P, Selbig J, Müller LA, Rhee SY, Stitt M. 2004. MAPMAN: a user-driven tool to display genomics data sets onto diagrams of metabolic pathways and other biological processes. *The Plant journal : for cell and molecular biology* **37**, 914–39.

Vandenabeele S, Vanderauwera S, Vuylsteke M, Rombauts S, Langebartels C, Seidlitz HK, Zabeau M, Van Montagu M, Inzé D, Van Breusegem F. 2004. Catalase deficiency drastically affects gene expression induced by high light in *Arabidopsis thaliana*. *The Plant Journal* **39**, 45–58.

Wan X-Y, Liu J-Y. 2008. Comparative Proteomics Analysis Reveals an Intimate Protein Network Provoked by Hydrogen Peroxide Stress in Rice Seedling Leaves. *Molecular & Cellular Proteomics* **7**, 1469–1488.

Yao Y, Sun Q. 2012. Exploration of small non coding RNAs in wheat (*Triticum aestivum* L.).

Plant Molecular Biology **80**, 67–73.

Zhang B. 2015. MicroRNA: a new target for improving plant tolerance to abiotic stress. *Journal of Experimental Botany* **66**, 1749–1761.

Zhou B, Fan P, Li Y, Yan H, Xu Q. 2016. Exploring miRNAs involved in blue/UV-A light response in *Brassica rapa* reveals special regulatory mode during seedling development. *BMC Plant Biology* **16**, 111.

Figure legends

Fig. 1. Effect of 1 h treatment with 10 mM H₂O₂ on the plants.

Fig. 2. Effect of H₂O₂ treatment on the endogenous H₂O₂ concentration. Values indicated with an asterisk are significantly different from that of detected at the starting time. Horizontal white and black bars indicate the light and dark periods, respectively.

Fig. 3. Effect of H₂O₂ treatment on the size and redox state of the ascorbate pool. A: Concentration of AsA and DHA and the percentage of DHA compared to ASA (the numbers above the columns). B: Half-cell reduction potential of the DHA/AsA couple. Values indicated with an asterisk are significantly different from that of detected at the starting time. Horizontal white and black bars indicate the light and dark periods, respectively. C: Control; T: Treated.

Fig. 4. Effect of H₂O₂ treatment on the size and redox state of the glutathione pool. A: Concentration of GSH and GSSG and the percentage of GSSG compared to GSH (the numbers above the columns). B: Half-cell reduction potential of the GSSG/2GSH couple. Values indicated with an asterisk are significantly different from that of detected at the starting time. Horizontal white and black bars indicate the light and dark periods, respectively. C: Control; T: Treated.

Fig. 5. Effect of H₂O₂ on the activity of antioxidant enzymes. A: catalase, B: ascorbate peroxidase, C: glutathione reductase and D: glutathione S-transferase. Values indicated with an asterisk are significantly different from that of detected at the starting time. Horizontal white and black bars indicate the light and dark periods, respectively.

Fig. 6. Expression of H₂O₂-responsive miRNAs determined by comparative transcriptome profiling. Expression changes of framed miRNAs were validated by qRT-PCR (Fig. 7).

Fig. 7. Time-course of the expression changes of miRNAs during 1-day H₂O₂ treatment. Horizontal white and black bars indicate the light and dark periods, respectively. Values indicated with an asterisk are significantly different from that of detected at the starting time.

Fig. 8. Expression patterns of miRNA target genes after 1-day H₂O₂ treatment. A: PMP – peroxisomal membrane protein (TC458412); B: RA - Ribulose-1,5-bisphosphate carboxylase activase (CK215494); C: UGE - UDP-glucuronate epimerase (CA697618); D: UCTH7 - Ubiquitin carboxyl-terminal hydrolase 7 (CA612693); E: β-CI - beta-carotene isomerase (Ta#S52543088); F: IAA6 - Auxin-responsive protein (Ta#S61781874); G: ACP - ADP, ATP carrier protein 1 (CA665835); H: GPDH: Glycerol-3-phosphate dehydrogenase (TC402657). Values indicated with an asterisk are significantly different from that of detected at the starting time. The correlation coefficients between the expression of miRNAs and their targets are given for the H₂O₂-treated samples. Horizontal white and black bars indicate the light and dark periods, respectively.

Fig. 9. Network of the H₂O₂-responsive miR818 family members and their target genes. The whole network of the H₂O₂-responsive miRNAs and their targets determined by degradome sequencing or bioinformatics tools is shown in the Suppl. Fig. S7. Squares: miRNAs; triangles: target genes identified by both degradome analysis and bioinformatics tools, circles: target genes identified by bioinformatics tools, green filling indicates decrease and red filling indicates increase in the target gene expression based on microarray data, grey filling indicates the lack of expression data. Continuous lines: cleavage of the target, dashed lines: translational inhibition. The colour of the lines indicates the strength of the interaction.

Fig. 10. Proposed regulatory network of H₂O₂, various components of the redox system, miRNAs, their target genes and metabolic processes.

Figures

Fig. 1. Effect of 1 h treatment with 10 mM H_2O_2 on the plants.

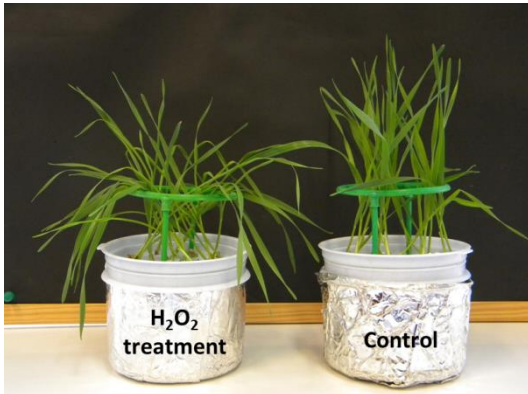


Fig. 2. Effect of H₂O₂ treatment on the endogenous H₂O₂ concentration.

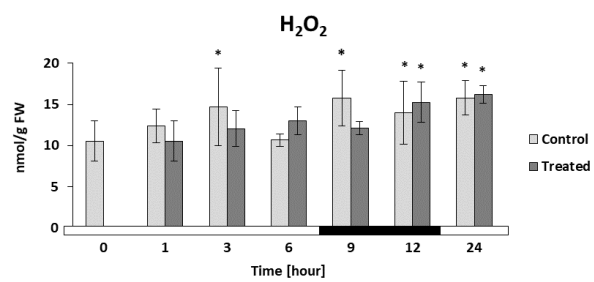


Fig. 3. Effect of H₂O₂ treatment on the size and redox state of the ascorbate pool.

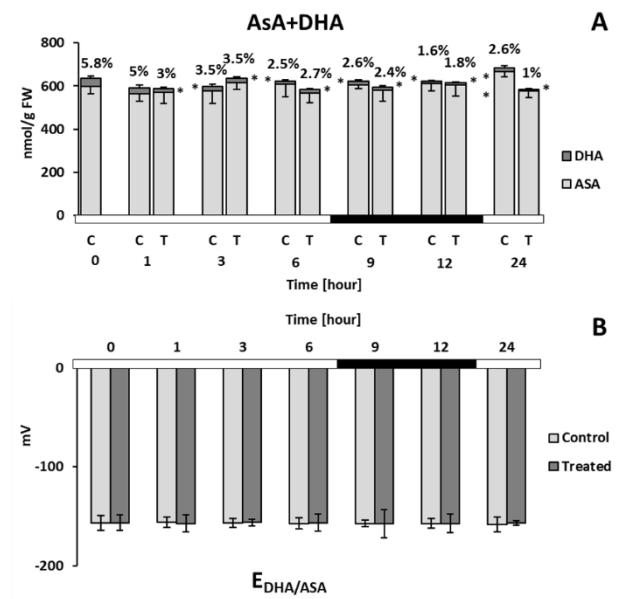


Fig. 4. Effect of H₂O₂ treatment on the size and redox state of the glutathione pool.

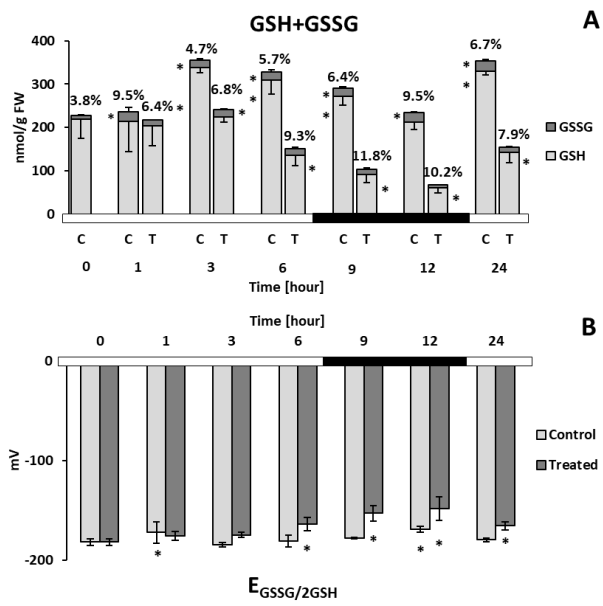


Fig. 5. Effect of H₂O₂ on the activity of antioxidant enzymes.

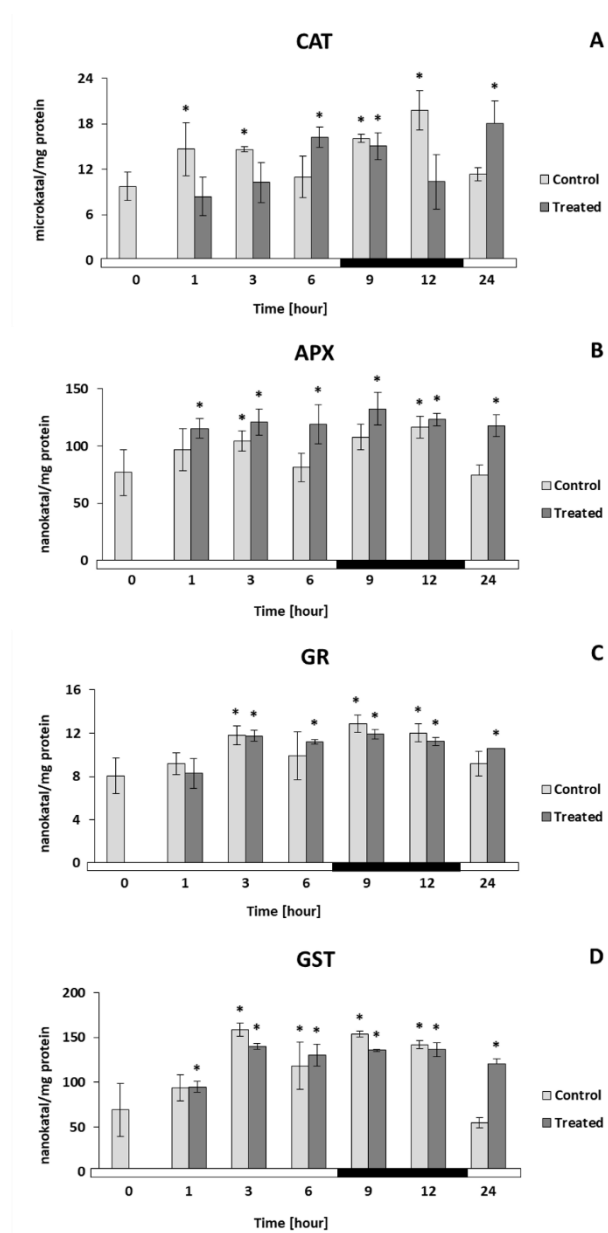


Fig. 6. Expression of H₂O₂-responsive miRNAs determined by comparative transcriptome profiling.

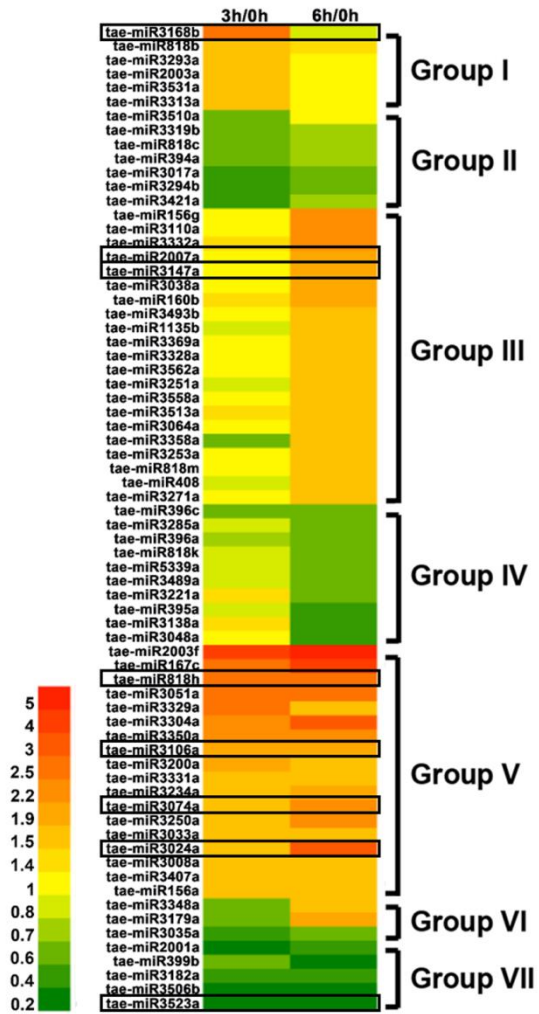


Fig. 7. Time-course of the expression changes of miRNAs during 1-day H₂O₂ treatment

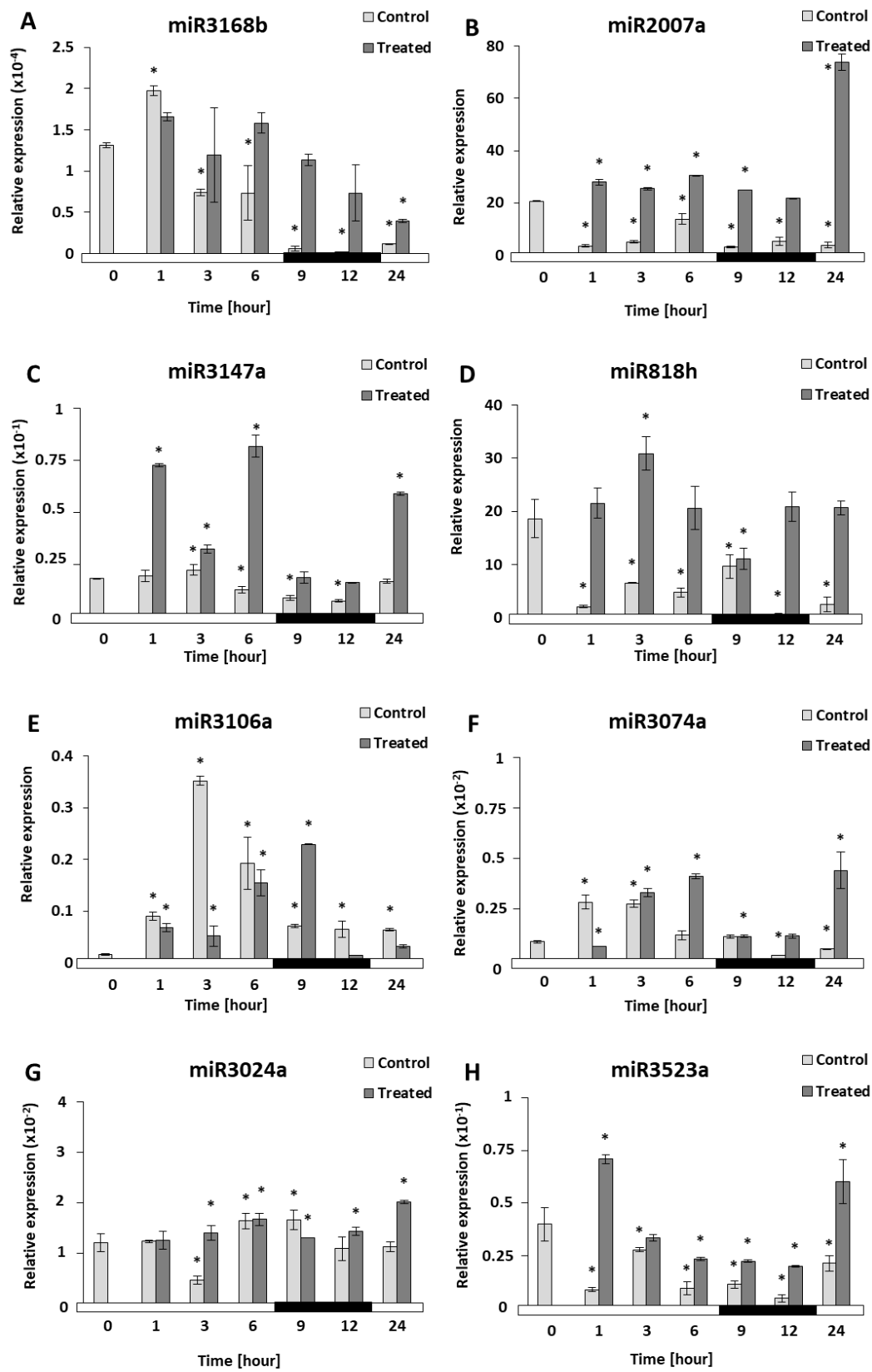


Fig. 8. Expression patterns of miRNA target genes after 1-day H₂O₂ treatment.

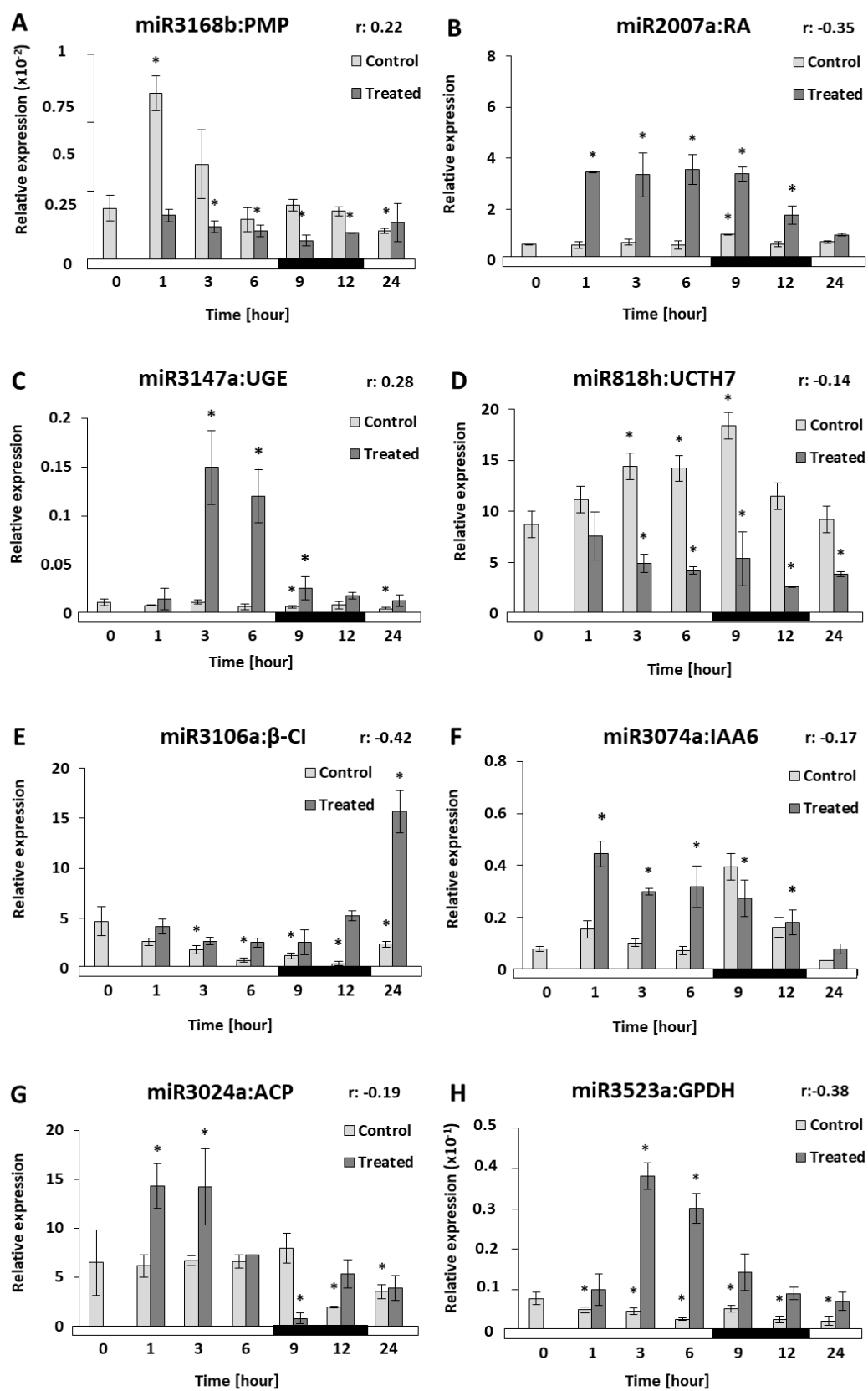


Fig. 9. Network of the H₂O₂-responsive miR818 family members and their target genes.

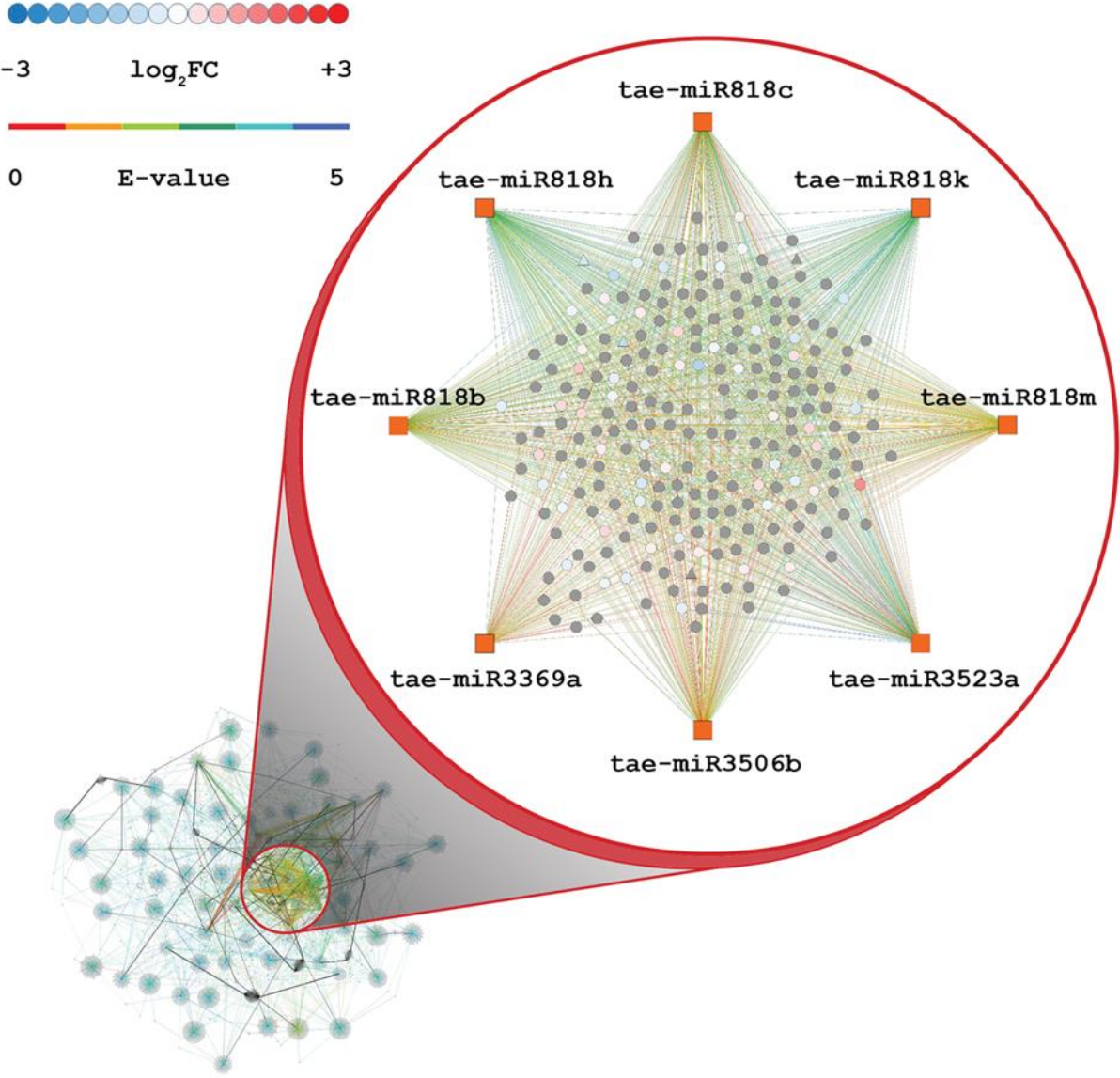


Fig.10. Proposed regulatory network of H₂O₂, redox system, miRNAs, their target genes and metabolic processes.

